

REPORT DOCUMENTATION PAGE

The public reporting burden for this collection of information is estimated to average 1 hour per response, including the time for reviewing the collection of information, sending comments regarding this burden estimate or any aspect of this collection of information, including suggestions for reducing the burden, to the Department of Defense, Executive Service Directorate (0704-0188). Respondents should be aware that notwithstanding any other provision of law, no person shall be subject to any penalty for failing to comply with a collection of information if it does not display a currently valid OMB control number.

PLEASE DO NOT RETURN YOUR FORM TO THE ABOVE ORGANIZATION.

1. REPORT DATE (DD-MM-YYYY) 31-12-2008		2. REPORT TYPE Final		3. DATES COVERED (From - To) 01-01-2006 - 31-12-2008	
4. TITLE AND SUBTITLE ABLATION AND PLASMA FORMATION DURING DIRECTED ENERGY TESTING				5a. CONTRACT NUMBER	
				5b. GRANT NUMBER FA9550-06-1-0393	
				5c. PROGRAM ELEMENT NUMBER	
6. AUTHOR(S) Iain D. Boyd				5d. PROJECT NUMBER	
				5e. TASK NUMBER	
				5f. WORK UNIT NUMBER	
7. PERFORMING ORGANIZATION NAME(S) AND ADDRESS(ES) University of Michigan 1320 Beal Ave Ann Arbor, MI 48109-2140				8. PERFORMING ORGANIZATION REPORT NUMBER	
9. SPONSORING/MONITORING AGENCY NAME(S) AND ADDRESS(ES) Air Force Office of Scientific Research 875 N Randolph St Arlington, VA 22203 Dr. John Schmisser/NA				10. SPONSOR/MONITOR'S ACRONYM(S) AFOSR	
				11. SPONSOR/MONITOR'S REPORT NUMBER(S)	
12. DISTRIBUTION/AVAILABILITY STATEMENT Approved for public release; distribution unlimited					
20090429207					
13. SUPPLEMENTARY NOTES					
14. ABSTRACT Continuous radio-wave telemetry is required during planned tests of directed-energy weapons systems in order to characterize in situ the effects of laser irradiation on different target materials. Unfortunately, the incident radiation can cause disruption of the radio signal during the directed-energy testing. Several phenomena associated with directed-energy impact can lead to communication path losses, such as ablation, charged particle emission, charring, and chemical changes in the target materials. Directed-energy impact on the target material leads to target heating and consequent ablation. A numerical model has been developed to describe the laser induced ablation of metal surfaces. The model describes the absorption of the laser energy by the metal and the resulting temperature rise in the surface. This temperature rise then induces ablation of the target material. Results for an aluminum target irradiated with a KrF laser were obtained. Temperature profiles in the target material and surface temperature changes are presented along with the ablation rate as a function of time as the aluminum target is irradiated. This report presents results for cases when laser energy absorption by the plasma plume created above the surface is not significant.					
15. SUBJECT TERMS Laser Ablation, Target Heating, Ablation Modeling					
16. SECURITY CLASSIFICATION OF:			17. LIMITATION OF ABSTRACT	18. NUMBER OF PAGES	19a. NAME OF RESPONSIBLE PERSON
a. REPORT	b. ABSTRACT	c. THIS PAGE			19b. TELEPHONE NUMBER (Include area code)

FINAL TECHNICAL REPORT

ABLATION AND PLASMA FORMATION DURING DIRECTED ENERGY TESTING

AFOSR GRANT FA9550-06-1-0393

Iain D. Boyd
Department of Aerospace Engineering
University of Michigan
Ann Arbor, MI 48109-2140

ABSTRACT

Continuous radio-wave telemetry is required during planned tests of directed-energy weapons systems in order to characterize *in situ* the effects of laser irradiation on different target materials. Unfortunately, the incident radiation can cause disruption of the radio signal during the directed-energy testing. Several phenomena associated with directed-energy impact can lead to communication path losses, such as ablation, charged particle emission, charring, and chemical changes in the target materials. Directed-energy impact on the target material leads to target heating and consequent ablation. A numerical model has been developed to describe the laser induced ablation of metal surfaces. The model describes the absorption of the laser energy by the metal and the resulting temperature rise in the surface. This temperature rise then induces ablation of the target material. Results for an aluminum target irradiated with a KrF laser were obtained. Temperature profiles in the target material and surface temperature changes are presented along with the ablation rate as a function of time as the aluminum target is irradiated. This report presents results for cases when laser energy absorption by the plasma plume created above the surface is not significant.

INTRODUCTION

Directed-energy impact on the target material leads to target heating and consequent ablation. The ablated material continues to expand, compresses the air and forms a shock wave in the air¹. Within the plasma and near the shock front, the combination of high air temperatures and the ablated material causes complex chemical reactions leading to ionization, recombination, and excitation. In addition, chemical reactions between the ablated material and air molecules are possible at these elevated air temperatures.

There have been a number of numerical models proposed to analyze the laser-solid interaction and ablation process^{11,12,14,15}. We developed a model based on a kinetic description of the Knudsen layer and a hydrodynamic description of the collision-dominated plasma region. Preliminary analysis of the ablation rate of various targets subject to directed-energy impact was performed. The ablation rate depends on the surface temperature as well as plasma density in the target vicinity². In this present paper, we report on an initial attempt

to apply this ablation model to a general case of an aluminum target being irradiated by a KrF laser in vacuum conditions. The model predicts the ablation rate and the depth of the resulting crater, as well as the temperature profile in the target material.

MODEL

A variety of models are available for the description of the laser-target interaction in laser ablation. In this study, we shall model laser ablation of metals in a vacuum using ns-pulsed lasers with irradiances in the 10^8 - 10^9 W/cm² range. The laser irradiances are chosen to produce the required fluence. Several processes will be analyzed in this model, including surface temperature rise, heat conduction, plasma density, ablation rate and crater depth.

SURFACE TEMPERATURE

A macroscopic scale description of the laser-solid interaction is used in this study, whereby the thermal heat conduction equation is used to analyze heating of the metal. This approach is valid for laser interaction with metals, in which case laser light is absorbed by interaction with electrons, and is then transferred to lattice phonons by collisions. For metals, the energy relaxation time is of the order of 10^{-13} s, and therefore for ns-pulsed laser beams we can assume optical energy is turned instantaneously into heat, allowing the application of the heat conduction equation³.

The temperature rise in the target material due to the laser beam will be computed from the following equation⁴,

$$c\rho \frac{\partial T(z,t)}{\partial t} = \nabla \{K(T(z,t)) \nabla T(z,t)\} + q_{laser}(z,t) \quad (1)$$

where c = specific heat of the material

ρ = material density

K = temperature dependent thermal conductivity

q_{laser} = heat source due to laser radiation.

The direction into the target is taken as the positive- z axis. The first term on the right-hand side represents the heat conduction in the metal. The heat source term in Eq. (1), which is due to the absorption of laser beam radiation, is given by

$$q_{laser}(z,t) = \mu(z)I(z,t) \quad (2)$$

where μ = absorption coefficient

$I(z,t)$ = laser beam irradiance as a function of time and position in the target

The laser beam will be absorbed by the metal as it travels through the target material, causing its intensity to drop. This change in the laser beam intensity is given by the Beer-Lambert law⁴,

$$I(z,t) = AI_o(t) \exp \left[- \int_0^z \mu(z,t) dz \right] \quad (3)$$

where A = surface absorptivity
 I_0 = irradiance of the incident beam

Laser irradiances in the range of 10^8 - 10^9 W/cm² will be considered in this study. The effect of evaporation of the metal surface is incorporated into the model in order to obtain an accurate description of the thermal field in the target material. Convection and radiation effects will be included in the future to better describe the heating effect of the laser.

PLASMA DENSITY

The plasma density at the surface can be determined if the equilibrium vapor pressure can be specified. The following relation⁵ gives the equilibrium vapor pressure at the surface as

$$\log_{10} p = 11.60 - 15880/T_0 \quad \text{where } T_0 = \quad (4)$$

temperature at the surface

The equation of state $p = n_0 k T_0$ can then be used to calculate the density at the surface.

ABLATION RATE

The ablation rate will be calculated using the kinetic model described in Keidar et al⁶. A schematic representation of the plasma and kinetic layers near the surface of the target is shown in Figure 1. In the kinetic region, using Anisimov's assumption⁷ that the velocity distribution function for the returned particles is $\beta f_1(V)$, where β is a proportionality coefficient, the relation of the heavy particle parameters at the outer boundary of the kinetic layer is given by the following set of equations.

$$\frac{n_0}{2(\pi d_0)^{0.5}} = n_1 V_1 + \beta \frac{n_1}{2(\pi d_1)^{0.5}} \times \{ \exp(-\alpha^2) - \alpha \pi^{0.5} \operatorname{erfc}(\alpha) \} \quad (5)$$

$$\frac{n_0}{4d_0} = \frac{n_1}{2d_1} \{ (1 + 2\alpha^2) - \beta [(0.5 + \alpha^2) \operatorname{erfc}(\alpha) - \alpha \exp(-\alpha^2)/\pi^{0.5}] \}$$

$$\frac{n_0}{(\pi d_0)^{1.5}} = \frac{n_1}{\pi d_1^{1.5}} \{ \alpha(\alpha^2 + 2.5) - 0.5\beta [\alpha(\alpha^2 + 2.5) \operatorname{erfc}(\alpha) - (\alpha^2 + 2) \exp(-\alpha^2)/\pi^{0.5}] \}$$

where $\alpha = V_1 / (2kT_1/m)^{0.5}$

$$d_0 = m / (2kT_0)$$

$$d_1 = m / (2kT_1)$$

$$\operatorname{erfc}(\alpha) = 1 - \operatorname{erf}(\alpha)$$

$$\operatorname{erf}(\alpha) = \text{error function.}$$

For relatively small plasma densities, we can assume that the plasma accelerates to the sound speed at the edge of the kinetic layer, and in this case the solution of the kinetic layer

equations (5) gives the plasma density at the edge of this layer as being equal to $0.34n_0$ and the temperature as $0.67T_0$. The ablation rate is then given by the relation¹³

$$G = mn_1V_1 \quad (6)$$

where m = mass of the particles

n_1 = plasma density

V_1 = velocity at the edge of the kinetic layer

Since we have assumed expansion to sound speed, the velocity at the edge of the kinetic layer is then given by

$$V_1 = \sqrt{2kT_1/m}$$

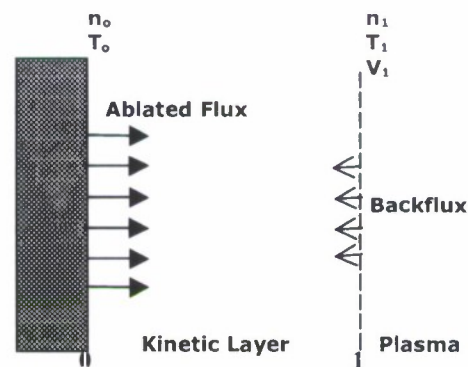


Figure 1 Schematic representation of kinetic layer near the surface

LASER PULSE

The laser pulse assumed in this study had a Gaussian profile with FWHM of 8 ns, and centered at 15 ns. Furthermore, a KrF laser was modeled, with wavelength, λ , of 248 nm. In this study, the laser fluence is chosen as the parameter, and the laser beam intensity is calculated to produce the required fluence. Fluences in the range of $3.0\text{-}8.0\text{ J/cm}^2$ were considered in this paper. An example of the laser beam profile is shown in Figure 2 for the case of 8.0 J/cm^2 .

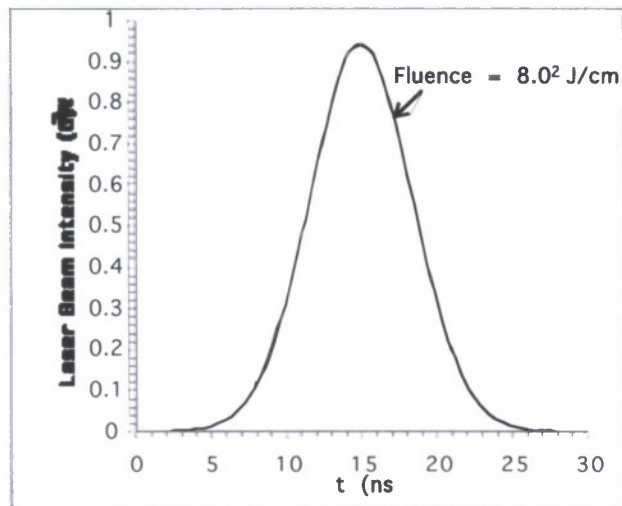


Figure 2 Laser beam intensity profile used in the model. This profile corresponds to a fluence of 8.0 J/cm^2

Table 1 Parameter values in the model with aluminum as the target material.

Specific Heat, c	$940.0 \text{ J kg}^{-1} \text{ K}^{-1}$ (solid), $1289.0 \text{ J kg}^{-1} \text{ K}^{-1}$ (liquid)
Mass Density, ρ	2700.0 kg m^{-3} (solid), 2375.0 kg m^{-3} (liquid)
Melting Point, T_m	933.5 K
Heat of Evaporation, H_{ev}	$10.8 \times 10^6 \text{ J kg}^{-1}$
Atomic mass, m	27 g mol^{-1}
Absorption Coefficient, μ	$5.7 \times 10^7 \text{ m}^{-1}$
Absorptivity, A	0.21

RESULTS OF THE MODEL

The laser model was applied to an aluminum target, with material properties as given in Table 1. Aluminum was chosen as the target because it is a material of interest and to allow for comparison of the results with other models.

TARGET HEATING

The aluminum target is initially at room temperature of 300 K . As a result of the incident laser beam, the target will be heated. The temperature distribution in the target material is plotted at several representative times in Figure 3. As expected, the temperature is maximum at the surface for all times.

Initially the temperature near the surface rises quickly as the laser beam intensity reaches its highest value at 15 ns . The maximum temperature is achieved at the surface several nanoseconds after the peak laser intensity. After this the surface temperature as well as the temperature in the target begins to drop as the amount of energy being absorbed is reduced.

The temperature gradients in the target also decrease and a smoother profile is observable at large times. It can also be observed that the heat conduction has penetrated to about 10 μm into the material in 100 ns.

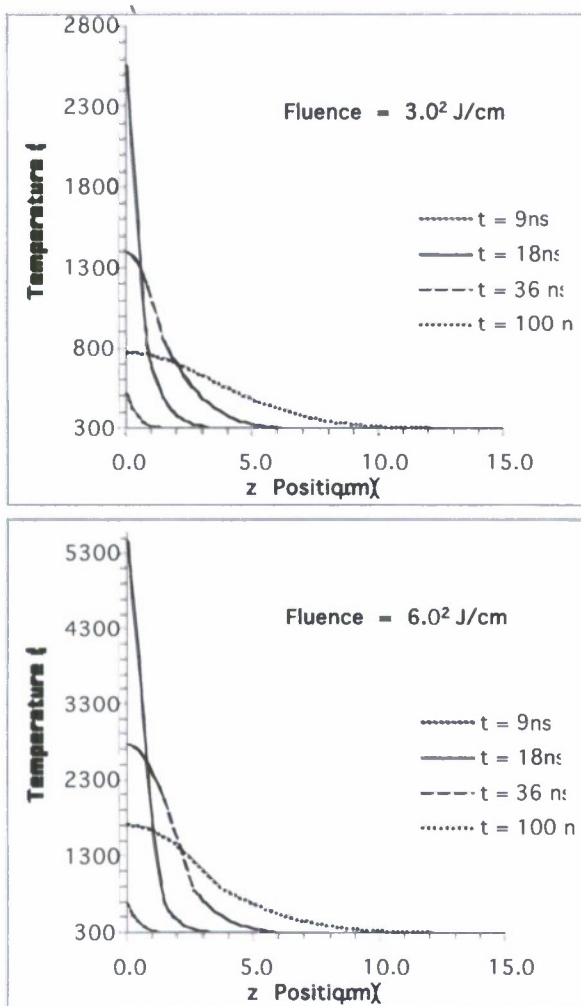


Figure 3 Calculated temperature profile in the aluminum target for a fluence of 3.0 J/cm^2 (a) and 6.0 J/cm^2 (b) as a function of time

SURFACE TEMPERATURE

The surface temperature profile as a function of time is plotted in Figure 4 for several laser fluences. Higher laser fluence results in a higher temperature rise at the surface, as expected. This is because more energy is absorbed by the target material. Figure 4 (a) shows the surface temperature variation with time for fluences of 3.0 and 3.3 J/cm^2 . It is found that a maximum temperature of 2880 K is obtained for a fluence of 3.3 J/cm^2 and 2560 K for the 3.0 J/cm^2 fluence case. After reaching a maximum about 6 ns after the peak laser intensity, the surface temperature drops off slowly as heat is transferred into the aluminum target.

Similarly, Figure 4 (b) shows that maximum surface temperatures of 3660 K, 5500 K and 6530 K we obtained for fluences of 4.0, 6.0, and 8.0 J/cm² respectively.

These results agree with results in Peterlongo et al.⁸, where a triangular laser beam profile was used instead. A maximum surface temperature of 2588 K is obtained about 5 ns after the peak laser intensity for a fluence of 3.0 J/cm². For 3.3 J/cm², the maximum surface temperature obtained was 2859 K. Amoruso⁹ used a square laser beam profile to study the ablation process of aluminum and obtained surface temperature profiles that qualitatively looked different than the profiles obtained here. This was due to the different laser beam profiles assumed. Nevertheless, maximum surface temperatures of about 2650 K and 4400 K were obtained for fluences of 3.0 and 6.0 J/cm². Mele et al.¹⁰ meanwhile used a KrF laser with Gaussian profile (FWHM of 18 ns) and obtained maximum surface temperatures of about 3150 K and 5200 K for fluences of 3.0 and 6.0 J/cm² respectively.

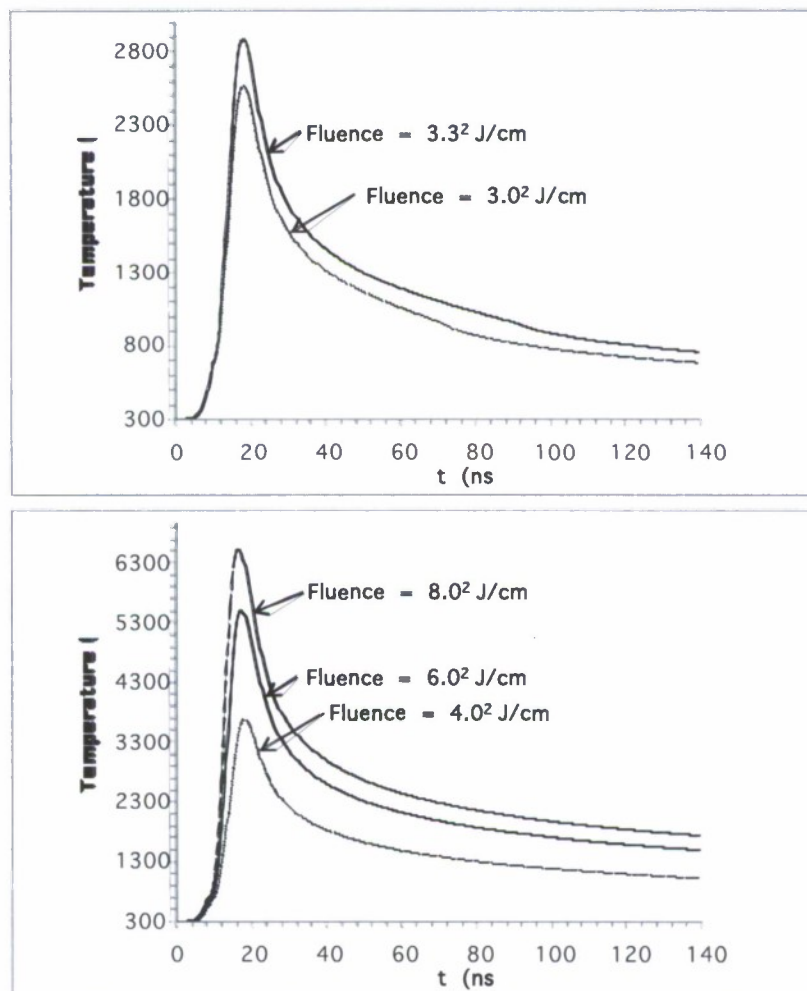


Figure 4 Calculated surface temperature profile in the aluminum target for a fluence of 3.0 and 3.3 J/cm² (a) and 4.0, 6.0 and 8.0 J/cm² (b)

ABLATION RATE

The heating of the aluminum target will cause the target material to start evaporating, and the ablation rate will generally increase as the surface temperature increases. The ablation rate of the aluminum during the laser irradiance is shown in Figure A. The results indicate that the ablation rate increases sharply as the target surface temperature rises, and begins dropping as the laser beam intensity drops and the surface temperature decreases. In fact, the vaporization of material is one of the factors causing the surface temperature to drop.

The results for ablation rate, shown in Figure 5 (a) indicates that a maximum ablation rate of $16.06 \text{ kg/m}^2\text{s}$ is obtained for a fluence of 3.0 J/cm^2 , while an ablation rate of $74.57 \text{ kg/m}^2\text{s}$ is obtained for a fluence of 3.3 J/cm^2 . Meanwhile, Figure 5 (b) shows ablation rates of approximately 22800 and 59400 $\text{kg/m}^2\text{s}$ are obtained for fluences of 6.0 and 8.0 J/cm^2 respectively. Therefore there are several orders of magnitude difference in the ablation rates for fluences in the range of 3.0 to 8.0 J/cm^2 . Nevertheless, the results for fluences above 6.0 J/cm^2 are not expected to be accurate as both Amoruso⁹ and Mele et al.¹⁰ indicate that laser absorption by the plasma plume becomes significant above this threshold.

Peterlongo et al.⁸ obtained a maximum ablation rate of $18.9 \text{ kg/m}^2\text{s}$ for a fluence of 3.0 J/cm^2 and $59.4 \text{ kg/m}^2\text{s}$ for a fluence of 3.3 J/cm^2 . This difference in maximum ablation rate is possibly caused by the different methods used to evaluate the rate of ablation. The kinetic approach used in this study is a more detailed and accurate model and therefore should give a better approximation.

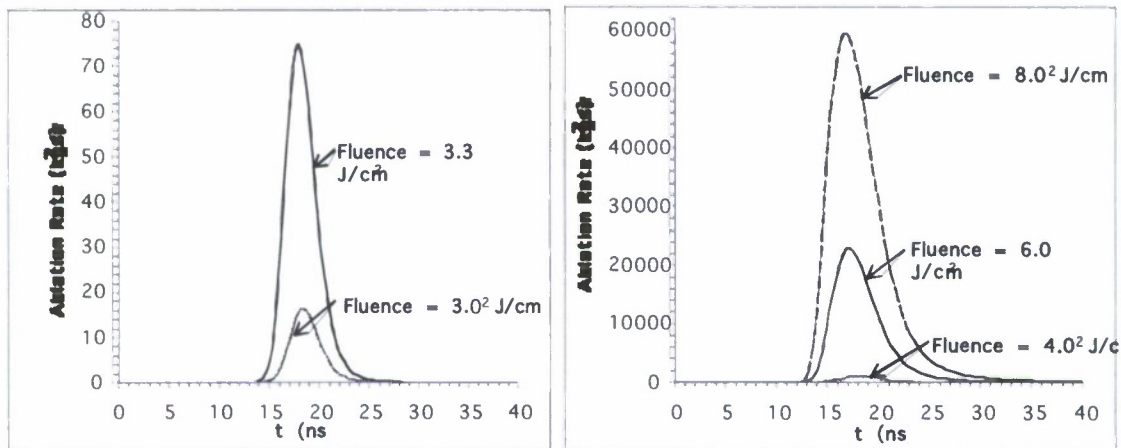


Figure 5 Ablation rate as a function of time for fluences of 3.0 and 3.3 J/cm^2 (a) and $4.0, 6.0, 8.0 \text{ J/cm}^2$ (b)

EVAPORATED DEPTH

The laser induced ablation of the aluminum target results in material loss from the surface. In an experimental setting, this would result in a crater around the laser beam incidence location. In this 1-D study, this material removal causes in the thickness of the target material to be reduced. The depth of evaporation is shown in Figure 6. This shows most of the change

in depth occurring between 12 ns and 33 ns after the beginning of the laser pulse irradiation. After that, as the ablation rate drops, the evaporation depth levels off.

Fluence of 3.0 and 3.3 J/cm² produce an evaporation depth of about 0.021 and 0.105 nm respectively, as shown in Figure 6 (a). Figure 6 (b) shows that fluences of 4.0, 6.0 and 8.0 J/cm² produce evaporation depths of 1.580, 45.00, and 132.2 nm respectively. Again there are several orders of magnitude difference between the evaporation depth for the fluences in consideration.

Mele et al.¹⁰ obtained evaporation depths of about 6.5 and 48 nm for fluences of 4.0 and 6.0 J/cm² respectively. This is generally in agreement with results of this present model. Bogaerts et al.¹² analyzed laser ablation for a copper target and found that for laser intensities in the range of 10⁸-10⁹ W/cm², the evaporation depth was in the range of 0-100 nm.

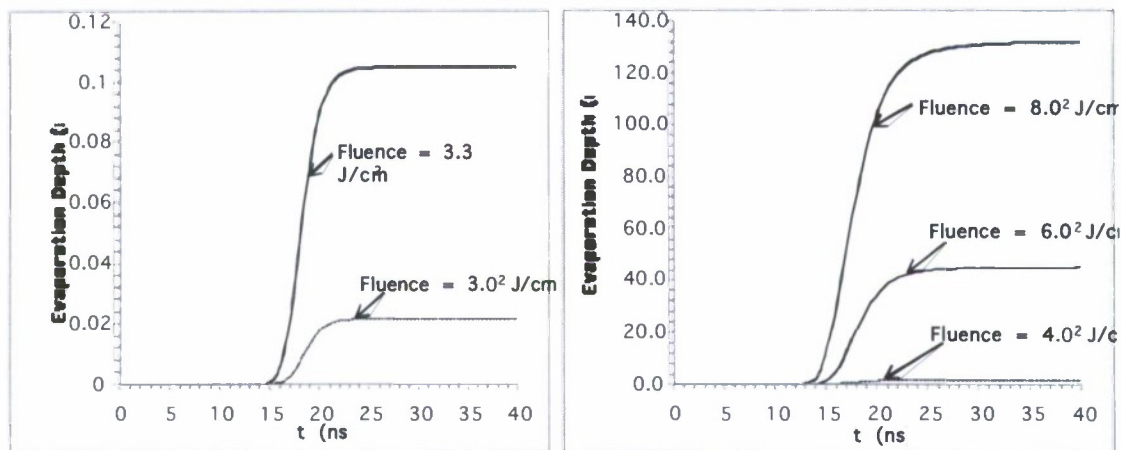


Figure 6 Evaporation depth as a function of time for fluences of 3.0 and 3.3 J/cm² (a) and 4.0, 6.0, 8.0 J/cm² (b)

CONCLUSION

This report has described a model for nanosecond pulsed laser ablation of an aluminum target in vacuum conditions for cases when the laser beam absorption by the plasma above the target is not significant. This model describes the laser-solid interaction that results in target heating and vaporization leading to ablation. The results include the temperature distribution in the aluminum target, the surface temperature profile, the ablation rate and the amount of evaporation.

Laser fluences in the range of 3.0-8.0 J/cm² were considered. Studies indicate that for fluences above this range, laser absorption by the plasma created by the ablation becomes significant and has to be taken into account. Results show that temperatures of 2560 K and 5500 K are obtained for fluences of 3.0 and 6.0 J/cm². Furthermore, 0.021 nm of aluminum was evaporated for a fluence of 3.0 J/cm² while 45 nm was evaporated for a fluence of 6.0 J/cm². The results show acceptable agreement with results of other analytical ablation

models, although the use of different laser beam profiles makes any accurate comparison difficult.

It should be reiterated that only after considering the plasma plume expansion above the target can accurate results be obtained for the higher fluences which are of interest. Nevertheless, this goal of this report was to demonstrate that the laser-solid interaction model presented here is acceptable for lower fluences. The results obtained using this ablation model, particularly the temperature, velocity and density at the edge of the kinetic layer will be used as boundary conditions to model the plasma plume expansion above the target in order to obtain accurate results for laser ablation at higher fluences.

REFERENCES

- ¹Radziemski, L.J. and Cremers, D.A., Laser-Induced Plasmas and Applications. Marcel Dekker, Inc. (1989)
- ²Keidar, M., Boyd, I.D. and Beilis, I.I., "On the model of Teflon ablation in an ablation controlled discharge," J. Phys. D: Appl. Phys. 34, (2001) 1675
- ³von Allmen, M., Laser Beam Interactions with Materials. Springer Heidelberg (1987)
- ⁴Semak, V.V. and Miller, T.F., "Modeling of Laser Charring and Material Removal in Fiberglass Materials," J. Directed Energy 2(1), (2006) 5
- ⁵Dushman, S., Vacuum Techniques. John Wiley & Sons, Inc. (1949)
- ⁶Keidar, M., Fan, J., Boyd, I.D. and Beilis, I.I., "Vaporization of heated materials into discharge plasmas," J Appl. Phys. 89(6), (2001) 3095
- ⁷Anisimov, S.I. Sov. Phys. JETP 27, (1968) 182
- ⁸Peterlongo, A., Miotello, A., and Kelly, R., "Laser-pulse sputtering of aluminum: Vaporization, boiling, superheating, and gas-dynamic effects," Phys. Rev. E 50(6), (1994) 4716
- ⁹Amoruso, S., "Modeling of UV pulsed-laser ablation of metallic targets," Appl. Phys. A 69, (1999) 323
- ¹⁰Mele, A., Guidoni, A.G., Kelly, R., Flamini, C. and Orlando, S., "Laser ablation of metals: Analysis of surface-heating and plume-expansion experiments," Appl. Surf. Sci. 109, (1997) 584
- ¹¹Yilbas, B.S., "Numerical approach to pulsed laser heating of Semi-Infinite Aluminum substance," Heat and Mass Trans. 31, (1996) 279
- ¹²Bogaerts, A., Chen, Z., Gijbels, R. and Vertes, A., "Laser ablation for analytical sampling what can we learn from modeling?," Spectrochimica Acta Part B 58, (2003) 1867
- ¹³Keidar, M., Boyd, I.D., Luke, J. and Phipps, C., "Plasma generation and plume expansion for a transmission-mode microlaser ablation plasma thruster," J. Appl. Phys. 96(1), (2004) 49
- ¹⁴Boardman, A.D., Cresswell, B. and Anderson, J., "An analytical model for the laser ablation of materials," Appl. Surf. Sci. 96-98, (1996) 55
- ¹⁵Leboeuf, J.N., Chen, K.R., Donato, J.M., Geohegan, D.B., Liu, C.L., Puretzky, A.A. and Wood, R.F., "Modeling of dynamical processes in laser ablation," Appl. Surf. Sci. 96-98, (1996) 14
- ¹⁶Tannehill, J.C., Anderson, D.A. and Pletcher, R.H., Computational Fluid Mechanics and Heat Transfer. Taylor & Francis (1997)